

IOWA STATE UNIVERSITY

Digital Repository

Graduate Theses and Dissertations

Iowa State University Capstones, Theses and
Dissertations

2017

Development of FEA models to study contusion patterning in layered tissue and the shaft loaded blister test

Christopher James Giuffre
Iowa State University

Follow this and additional works at: <https://lib.dr.iastate.edu/etd>



Part of the [Aerospace Engineering Commons](#)

Recommended Citation

Giuffre, Christopher James, "Development of FEA models to study contusion patterning in layered tissue and the shaft loaded blister test" (2017). *Graduate Theses and Dissertations*. 15523.
<https://lib.dr.iastate.edu/etd/15523>

This Thesis is brought to you for free and open access by the Iowa State University Capstones, Theses and Dissertations at Iowa State University Digital Repository. It has been accepted for inclusion in Graduate Theses and Dissertations by an authorized administrator of Iowa State University Digital Repository. For more information, please contact digirep@iastate.edu.

Development of FEA models to study contusion patterning in layered tissue and the shaft loaded blister test

by

Christopher James Giuffre

A thesis submitted to the graduate faculty

in partial fulfillment of the requirements for the degree of

MASTERS OF SCIENCE

Major: Engineering Mechanics

Program of Study Committee:
Ashraf Bastawros, Major Professor
Wei Hong
Jason Gillette

Iowa State University
Ames, Iowa
2017

Copyright © Christopher James Giuffre, 2017. All rights reserved.

TABLE OF CONTENTS

	Page
LIST OF FIGURES	iv
LIST OF TABLES.....	v
NOMENCLATURE	vi
ACKNOWLEDGMENTS	vii
ABSTRACT.....	viii
CHAPTER 1 INTRODUCTION	1
Background	1
Influence of Rounded Edges on Contusion Size	2
Shaft Loaded Blister Test	3
Research Objectives	3
Thesis Structure	4
CHAPTER 2 LITERATURE REVIEW	6
Material Modelling and Parameters	6
Contusion and Tissue Damage FEA.....	9
Experimental Analysis of Human Contusions.....	11
Matching Contusions and Object	12
Mechanics of Contusion Formation and Dissipation	12
CHAPTER 3 INFLUENCE OF ROUNDED EDGES ON CONTUSIONS	14
Model Parameters	14
Model Response	15
Contusion Formation and Patterning.....	20
CHAPTER 4 SHAFT LOADED BLISTER TEST	25
Introduction	25
Model Setup	26
Stationary Crack Calculations	29
Moving Crack Calculations	34
Parametric Studies	37

CHAPTER 5	CONCLUSION	41
Summary.....		41
Simulation Uses.....		42
Simulation Limitations		43
Future Work.....		43
REFERENCES		45

LIST OF FIGURES

	Page
Figure 1 Contact Pressure Distribution [1]	2
Figure 2 FEA Model	15
Figure 3 Force-Displacement Curve for Sweep of Objects	16
Figure 4 FEA Contact Pressure Distributions.....	17
Figure 5 Indentation Pileup.....	19
Figure 6 Contusion Energy Analysis	21
Figure 7 Contusion Measurements	22
Figure 8 Contusion Dimensions.....	23
Figure 9 Contusion Dimensions for a Single Object	24
Figure 10 SLBT Geometry	26
Figure 11 SLBT Interactions.....	28
Figure 12 Bi-Linear Traction-Separation Curve.....	28
Figure 13 Calculated vs. FEA Displacement	31
Figure 14 G Calculations with FEA Solution	33
Figure 15 Model Response with Propagating Crack	35
Figure 16 G Calculations for Propagating Crack.....	36
Figure 17 Parametric Sweep of Thickness, Substrate Material, and Boundary Conditions	39
Figure 18 Parametric Sweep of Plug Radius	40
Figure 19 Parametric Sweep of Crack Length.....	41

LIST OF TABLES

	Page
Table 1 Summary of Constitutive Laws Used in Literature to Model Human Tissue	7
Table 2 Summary of experimental values of μ for skin and adipose tissue [11, 12]	9
Table 3 Model Parameters	14
Table 4 SLBT Model Parameters	27

NOMENCLATURE

CZM	Cohesive Zone Modelling
FEA	Finite Element Analysis
FEM	Finite Element Method
SLBT	Shaft Loaded Blister Test

ACKNOWLEDGMENTS

I would like to thank my major professor, Dr. Ashraf Bastawros, for everything he has done to help support me over the course of the past 2 years. His guidance and knowledge has been invaluable as I develop as both an engineer and scientific researcher.

I would also like to thank Dr. Wei Hong, and Dr. Jason Gillette for serving on my committee. Their knowledge of specific areas of the research has been invaluable source when learning about and working on these problems.

In addition, I would like to thank my parents for their endless support during my time at Iowa State University and for being my rock when I needed them the most. Finally I would like to thank all of my friends for their support, encouragement, and companionship has made my time at Iowa State University a wonderful experience.

ABSTRACT

In the natural world there is no such thing as a perfectly sharp edge, either thru wear or machining imprecision at the macroscopic scale all edges have curvature. This curvature can have significant impact when comparing results with theory. Both numerical and analytic models for the contact of an object with a sharp edge predict infinite stresses which are not present in the physical world. It is for this reason that the influence of rounded edges must be studied to better understand how they affect model response.

Using a commercial available finite element package this influence will be studied in two different problems; how this edge geometry effects the shape of a contusion (bruise) and the accuracy of analytic models for the shaft loaded blister test (SLBT). The contusion study presents work that can be used to enable medical examiners to better determine if the object in question was capable of causing the contusions present. Using a simple layered tissue model which represents a generic location on the human body, a sweep of objects with different edges properties is studied using a simple strain based injury metric. This analysis aims to examine the role that contact area and energy have on the formation, location, and shape of the resulting contusion. In studying the SLBT with finite element analysis and cohesive zone modeling, the assessment of various analytic models will provide insight into how to accurately measure the fracture energy for both the simulation and experiment. This provides insight into the interactions between a film, the substrate it is bonded to and the loading plug. In addition, parametric studies are used to examine potential experimental designs and enable future work in this field. The final product of this project provides tools and insight into future study of the effect rounded edges have on contact and this work enables for more focused studies within desired regimes of interest.

CHAPTER 1. INTRODUCTION

Background

In nature there are no perfectly sharp edges, unless you are working at the atomistic level. At the macro scale of millimeters and meters, the edges of objects have some level of curvature. This is due to a number of factors including imperfect machining and material removal over time. Sharp edges represent a number of issues when it comes to analytic solutions and numerical simulation. In the linear-elastic solution to a flat punch where the edge of the punch and substrate meet there is a theatrical infinite stress. While this is not possible in an experiment, the stress in this region is often much higher and plasticity is involved. This infinite stress is also present in linear-elastic finite element simulations (FEA) and pose significant issues when simulating this type of contact. It is for this reason that when simulating contact, an edge fillet will be applied to reduce this stress and allow the simulation to converge.

The influence and consequences of having this rounded edges have been studied in great detail for linear-elastic contact cases. Solutions have been develop for this problem using various techniques to solve the complex Muskhelishvili potential [1]. This work has resulted in solutions for internal stress and strain fields as well as the contact pressure distribution. The results of the work done by Ciavarella et al. is shown in Figure 1, for a range of edge fillets from a hemispherical object to a near sharp edged solution. When the object is hemispherical, the solution outputs the same results as Hertzian contact while it is clear the effects that the edges have on the contact pressure distribution. As the edge fillets get smaller, the peaks approach the width of the object and the peak pressure grows.

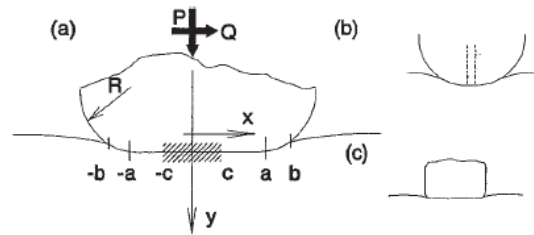
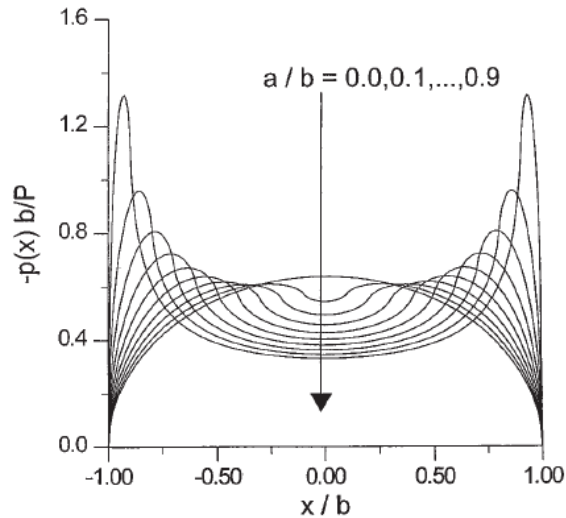


Fig. 1 (a) Geometry of indenter, (b) near-circular limit, (c) near flat-ended punch limit

Figure 1. Contact Pressure Distribution [1]

The influence of these changes of the edge fillet show interest in several different research areas. In this work two of these areas will be explored; the effects that rounded edges have on the initial shape of a contusion and the study of flat capped punches when used to conduct the shaft driven blister test. The study and development of finite element analysis models and simulations for these two problems will allow for more analysis of experimental data and the validation of analytic models.

Influence of Rounded Edges on Contusion Size

Contusions are among the most prevalent injuries and are often of significant importance in forensic cases where they can be crucial evidence. These injuries are indicative of blunt force trauma on soft tissue and can be telltale markings of abuse or violent crime. Due to the energy required to rupture the capillaries and cause blood to flow into the tissue, the injury can be in any tissue layer including the dermis, subcutaneous adipose, and muscle. Due to the violent nature that is often associated with contusions, there is a chance that patterns in the injury will exist which can help deduce the object that was used. To have a pattern be left by the impact a number of factors need to be taken into account including the area of the body, impact energy,

contact area, and a number of individual biological factors. Even with all of this taken into account, it is near impossible to predict the coloration and intensity of the injury. For this reason, the studies shown will only make statements about the overall size, location, and patterning of the potential injury.

Shaft Loaded Blister Test

The blister tests is an experimental method for determining the interfacial fracture energy of a film and substrate combination. This test has been developed since its inception in the 1960's to now where it has multiple solutions for the fracture energy based on the deformation mechanics in the film. Throughout this work, we are looking to apply FEA to study the accuracy of these solutions when the film being studies is ice and it cannot be considered a classical thin film. This work is of importance since the build-up and removal of ice is of great importance and interest in the aerospace community. As ice grows on the lifting surfaces of aircraft during flight the aerodynamic properties and aircraft performance are greatly effected in a negative manner. This decrease in the aircrafts ability to maneuver and generate lift creates a safety concern for all those involved. For this study a FEA model is developed, both stationary and moving cracks will be studied to determine the best method of determining the fracture energy. With the stationary crack, the J integral was used to compare values with the analytic solutions. For the moving crack, the fracture energy was compared to the input and analyzed until the damage zone reached the end of the interface.

Research Objectives

The objective of this thesis is to develop an understanding of the mechanics of the two stated problems using a commercial finite element package. Such understanding will allow for better and more focused research in the future and tools which will allow for the validation of

new and existing analytical solutions. For the contusion studies, it is important that only size, location, and basic features are discussed as properties like color and intensity are near impossible to predict with basic models. This work is designed to allow for basic predictions on generic puck models composed of various layers of tissue which can be associated with various places on the human body. This work will be used to provide basic predictions which will allow for more focused work when more complex location specific models are used for the same type of research.

The shaft loaded blister test simulations are designed to help with experimental design and the validation of analytic models. Using a simple axisymmetric model, data can be produced and examined with the goals of fine tuning experimental design to help capture the desired data. Using this model, it is possible to validate and determine the accuracy of several different simple analytical models which can be used on future simulations and experiments. With this work complete, studies can now be conducted on more complex substrate geometries and new factors such as surface roughness can be examined in great depth on a proven platform.

Thesis Structure

This thesis is organized into five chapters which encompass the work done to develop a basic understanding of the effects that rounded edges have on contusion patterning and the shaft loaded blister test. They will present the extent of current literature, discussion of modelling procedures, results for both the model response and measurements of important features. A brief description of the chapters follows:

Chapter 2: Literature Review – In this chapter, the current literature for the modelling, human testing, and mechanics of contusion formation are reviewed. This chapter is only focuses

on contusions due to the volume of work that needs to be examined to better understand this problem.

Chapter 3: Influence of Rounded Edges on Contusions – This chapter presents the methods, modelling techniques, model response, and findings about various contusion features. The required energy, contact area, location, and size of the predicted contusion are presented.

Chapter 4: Shaft Loaded Blister Test – This chapter focuses on the modelling and validation of analytic solutions for the SLBT experiment. A brief review of the experiment is included as well as necessary fracture mechanics concepts.

Chapter 5: Conclusion – This chapter discusses the uses of the models and solutions as well as current modelling limitations. Future work is discussed for the models and analytic solutions.

CHAPTER 2: LITERATURE REVIEW

The study of contusion formation and evolution has become a greater applications across multiple fields of study. This draws interest from engineers and scientist as a problem regarding non-linear material modeling, the mechanics of layered solids, finite element analysis, and damage modelling. There are medical applications and insight into how the human body is damaged and the resulting biological responses. The complex interaction that determines contusion formation and inflammation is still relatively unexplored and currently described in a qualitative manner. Finally there is significant legal implications especially with regards to homicide, assault, and abuse cases [2]. The ability to match contusions with the object in a scientific manner would provide invaluable evidence in court. All of these research avenues represent significant advancement in each field.

Material Modelling and Parameters

When it comes to modelling human tissue, the first of many hurdles is determining which of many different applicable constitutive laws best describe the complex stress-strain relation and near incompressibility of biological tissues. In the literature, several different yet common models have been used and can be found in Table 1. In addition to these, custom constitutive laws have been used in specialized situations [3].

Table 1. Summary of constitutive laws used in literature to model human tissue

Source	Dermis (skin)	Adipose (Fat)	Muscle	Viscoelastic Model
4	Single Term Ogden			
5	Single Term Ogden			
6	Linear Elastic	Neo-Hookean	Neo-Hookean	Prony Series for Adipose and Muscle
7	Linear Elastic	Linear Elastic	Linear Elastic	
8	Single Term Ogden	Single Term Ogden	Single Term Ogden	
9	Single Term Ogden	Single Term Ogden	Single Term Ogden	Prony Series

From this table, it is clear that the use of a single term Ogden material is by far the most common constitutive law used, especially as the literature approaches present day. The Ogden constitutive law was developed to better describe the behavior of incompressible hyperplastic material. With certain assumptions, this constitutive law can be reduced down to Mooney-Rivlin or Neo-Hookean constitutive laws however these assumptions results in no longer capturing the desired material response. The inputs for a Ogden material are two or three material parameters; μ_i , α_i , and D_i . For the single term Ogden material, the D term is not present and N is set to 1. To relate these inputs to material behavior, the single term Ogden material is defined using the strain energy potential and is expressed as the following equation [10]:

$$U = \sum_{i=1}^N \frac{2\mu_i}{\alpha_i^2} \left(\bar{\lambda}_1^{\alpha_i} + \bar{\lambda}_2^{\alpha_i} + \bar{\lambda}_3^{\alpha_i} - 3 \right) \quad 2.1$$

Where:

$$\bar{\lambda}_i = J^{-\frac{1}{3}} \lambda_i \text{ deviatoric principal stretch} \quad 2.2$$

To determine these values for human tissue, there are several difficulties that are not encountered when studying more traditional non-linear materials such as polymers and rubbers. The testing of living human tissues is very difficult and often impossible to conduct due to the difficulties with gaining permission to carry out the study. This means that for the majority of properties reported in the literatures are results from experiments done on animal tissues, specifically porcine (pig) tissues. These values are still very hard to determine and often require highly specialized testing methods and equipment. For the studies mentioned in Table 1 that use the single term Ogden model for skin and fat the values come from select studies by researchers at University of Cambridge UK [11, 12]. The results of from these studies form the parameters for current models which contain skin and adipose tissue layers. The values detailing muscle tissues are taken from various studies based upon the use in the model. To determine the adipose and skin properties, compression tests were conducted over various strain rate regimes. It was found that only the value of μ is rate dependent. In Table 2 the values for adipose and skin can be found along with the method used and applicable range strain rate.

Table 2. Summary of experimental values of μ for skin and adipose tissue [11, 12]

Regime	Strain Rate Range $\dot{\epsilon}$ (s^{-1})	Skin μ (kPa)	Adipose μ (kPa)	Experimental Method
Low	$2 \cdot 10^{-3} - 0.2$	0.4	400	Screw-Driven Test Machine
Intermediate	20 – 260	1.7	2200	Servo-Hydraulic Test Machine
High	1000 – 5700	1120	7500	Split Hopkinson Pressure Bar

The values for muscle have also been experimentally determined, but due to the active nature of the tissue and the desire to keep the studies as simple as possible they were not included. For the various studies that include muscle tissue, the material parameters usually correspond to the response of relaxed muscle, but this is a significant assumption to be made when trying to model trauma and damage.

Contusion and Tissue Damage FEA

As commercial finite element packages have expanded the available capabilities to include tools such as Ogden materials and interface mechanics, they have been used to simulate various configurations of layered human tissue. These simulations can be divided into several broad categories including impact loading and thoracic injury, tissue damage modelling, hierarchical modelling, and metric development. Each of these models is designed to examine a specific aspect of injury mechanics and tissue modelling.

There is a large portion of the literature which is devoted to the development of models with the intent to study how stresses travel through various layers of tissue and bone [13, 14]. Both Shen and Roberts studies both focus on the simulation of human thorax models. Both groups modeled not only the soft tissue but also rib structures and internal organs. Due to the

complexity of the interactions of the various components only simple constitutive relations were used. Both models used basic damage analysis to determine the extent of damage to the model. Due to the large size of these models and focus on overall damage, they provide minimal insight into contusion mechanics.

Moving closer to the simulation of contusions is the work done which studies deep tissue injuries using stress damage laws which uses a slice model to try and determine the damage done to tissue when lying on rigid surfaces for an extended time period[6]. Using an MRI scan to create a patient-specific model, this model has the ability to directly compare simulation results with a known injury. Using a custom damage law, this work shows that using hyper-elastic constitutive laws and a proven damage model, the ability exists to predict injury with little known about the initial conditions.

In a series of studies done to study the FEA was used to examine the effects of loading on a model of the human arm [7, 8]. Using a hierarchical model, with the largest model being different layers of tissue and the smallest being a single capillary, a stress based metric was used to determine when the capillary would rupture which would lead to subsequent contusion formation. Using linear elastic constitutive laws in Huang and Ogden materials in Grosse, a pressure distribution was directly applied to the outer layer of the skin which was then transmitted between the various submodels. Using their stress metric, it was determined that at sufficiently large yet reasonable loads a contusion would be present. However, the observations from the model can only yield details about the presence of a contusion with no information regarding extent of the contusion or severity. As noted in their work, since this model looks at a single capillary in a specific orientation limited conclusions can be made from this work.

Finally, there are models which look to develop metrics for contusions using more general engineering measurements. In combination with experiments performed on rats that had undergone a posterolateral thoracotomy so that load can be directly applied to the lung [8]. Using computed tomography (CT) to measure the damage 24 hours after the experiment, the damaged and contusion parameters were measured. Using a previously developed model and custom constitutive law, the loading was recreated in a dynamic FEA analysis. Based upon the parameters known from the CT scan, 11 different metrics were evaluated for accuracy. It was found for explicit simulations the product of the maximum principal strain and strain rate provided the best correlated metric. For standard simulations, the maximum principal strain provided the best correlated metric.

Experimental Analysis of Human Contusions

Due to various ethics constraints on instigating contusions on living subjects, the field is very small and the results suspect at best. Data is available in a couple of studies with two very different objectives. In Desmoulin et al [15], various impacts were made against the shin and calf of a healthy adult human. Measurements of the impact energy, peak force and contact area are used to help characterize various cut off values for the presence of contusions. In their findings, impact energy was found to be the best metric to determine the presence of a contusion. In addition to these measurements, data is presented regarding the size, color, and shape of the contusions present 24 hours post impact. In Pilling et al [16], a suction technique was used to produce uniform bruises in various participants. Using this technique, multiple bruises could be created and then tested against visual inspection to determine age. It was shown that using the coloration of the bruise, it is nearly impossible to accurately date the bruise. These findings are

corroborated with several other studies that show that color is a highly inaccurate method for determining age.

Matching Contusions and Object

The study of matching an object with the wound it inflicted is known as photogrammetry. Currently used by creating a 3D or 2D model of the object and matching against images of the injury. In the studies [17, 18], this has been shown to work for both 2D and 3D cases. However, this methodology is not without limitations and shortcomings. The first is that you have to start with both a good idea of what the object is if not the exact object. In both cases, the object that caused the contusion was well known and easily modeled in basic CAD software. The geometry of the object in both cases was flat which leads to the ability to overlay the CAD model on top of the contusion. As this method has evolved over time, the ability to overlay the contusion on a 3D surface which represents the contours of the injured area. In the studies conducted it is shown that good agreement between the object and contusion can be found. However, this was done on cadaver subjects and the contusions did not have the time to develop and change over time. This work represents what is currently being done to match a contusion with the object that caused it.

Mechanics of Contusion Formation and Dissipation

From a medical perspective, contusions are the result of capillary rupture and the resulting pulling of hemoglobin around the injury site. After the injury occurs the contusion will undergo a number of changes including shape, intensity, and color. Although contusions can happen immediately, there is a delay of approximately 24 hours before the contusion is considered fully formed. It is for this reason measurements of contusion parameters are taken 24 hours post injury. In addition to contusions, there is the possibilities of other injuries present

including abrasions, lacerations, and inflammation. While all of these injuries can be related and mechanics intertwined, the mechanics of bruising can be broken down into several distinct phenomena.

Finally there has been research done on the mechanics of contusion diffusion and dissipation using basic physical phenomena [19]. In their work the contusion is broken down into two different components: hemoglobin and bilirubin. For the duration of the simulations, both components are subject to diffusion via Fick's Law. This means that over time, the components will flow from regions of high concentration to low concentration. Both components are uncoupled when being subjected to Fick's Law and are driven by different constants. Due to the hemoglobin coming from a ruptured capillary, there will also be pressure driven diffusion. Following Darcy's law, the hemoglobin is subjected to diffusion due to the difference in pressure.

In addition to these diffusion laws, the concentration of hemoglobin and bilirubin is affected by chemical reactions. Both are subjected and coupled by enzyme kinetics by way of the Michaelis-Menten mechanism. This mechanism describes the conversion of a substrate (hemoglobin) to a product (bilirubin). This process can be represented as a chemical reaction using the following chemical equation. Finally, the bilirubin will leave the tissue through the lymphatic system by use of a zero order reaction kinetics which simply divides the concentration of bilirubin by a constant factor and removes that from the system (Stam 2010).

CHAPTER 3: INFLUNCE OF ROUNDED EDGES ON CONTUSIONS

Model Parameters

As discussed in the previous section, several different models have been used to simulate contact with layered human tissues. Models have been based off of medical images taken from healthy and statistically average human subjects [20]. These assumptions allow for the simplifications of the model which significantly decrease computational time. Based on assumptions in the published literature for this work the model used was a multi-layered puck model similar to the work in the literature [9]. Using this modelling platform allowed for easy parametric studies. Thickness dimensions were based off of both measurements taken from a healthy adult MRI and confirmed by the literature [9]. Width dimensions are such that the stresses have no interaction with the outer boundary. In Table 3 all of the major parameters of the model are given including tissue layer dimensions and material parameters. Figure 2 shows the model and parts labeled so the scale of the different dimension can be visualized. The object used to indent the surface is 80 mm in diameter which is approximately the diameter of a regulation softball. The layers of tissue were tied together via constraints as done in the literature [9].

Table 3. Model Parameters

Layer	Thickness (mm)	Width (mm)	μ (kPa)	α
Dermis (Skin)	3	130	2200	12
Adipose (Fat)	12	130	17	23
Bone	13.5	130	45800000	25

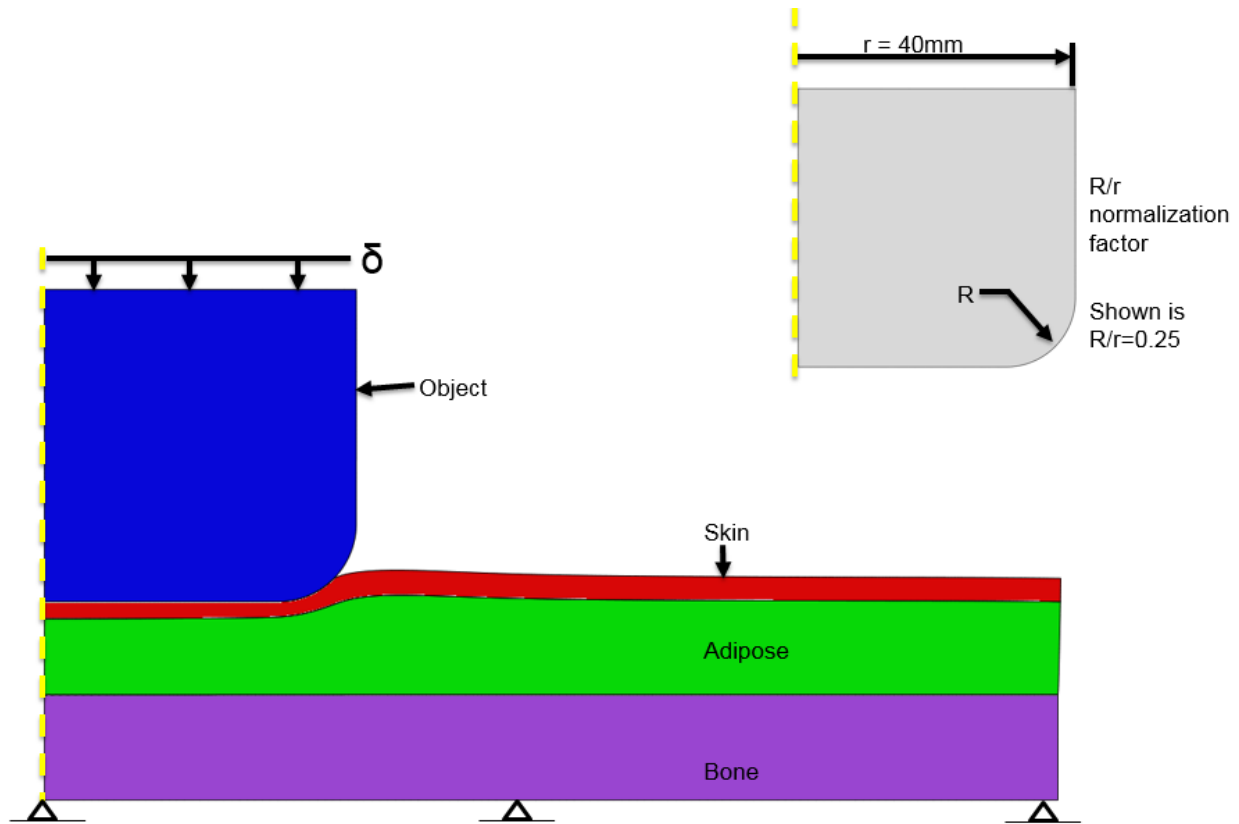


Figure 2. FEA Model

In order to examine data from multiple objects, a normalization factor must be selected which captures the important length scales of the problem. For this work, a normalization of R/r was selected and will be used when displaying data from various simulations. This allows for comparison across multiple objects and will further help to determine the dominate length scales of the problem.

Model Response

Figure 3 shows various force-displacement curves for a sweep of edge filets, R . As the edge of the object approaches a sharp edge, the model responds in a much stiffer manner. The model with the sharpest edge was run to a lower displacement due to computational instability in models where near infinity stress fields are present. This graph shows that the object radius has a

major implications on the response of the tissue. As the object goes from sharp edged to hemispherical, the displacement require to reach certain force levels can be increased from 1 mm to 5 mm. This shows the differences in contact profile and stresses which will in turn effect the contusion area and energy required to achieve the strain metric.

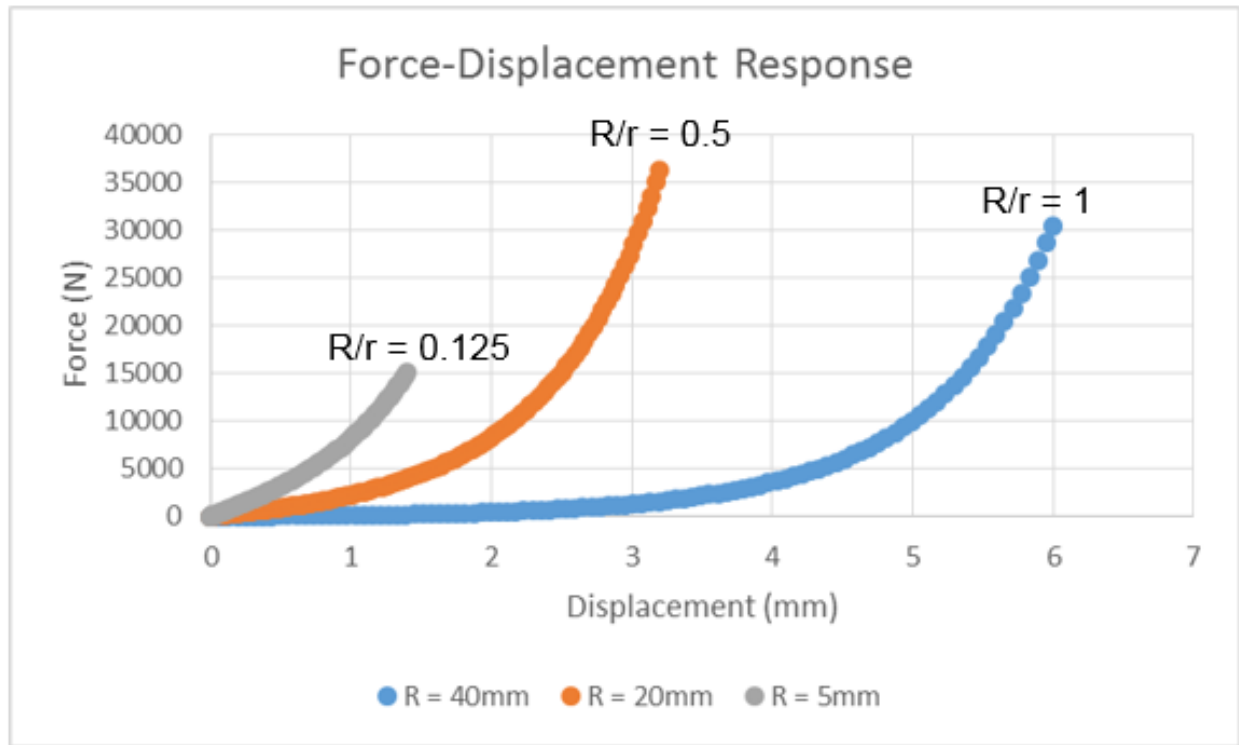


Figure 3. Force-Displacement Curve for Sweep of Objects

Secondly the contact stress curves for indentations of the total model were analyzed. Due to the complex nature of the material response in conjuncture with the layered nature of the model no analytic models exist to predict these loadings. During this analysis two different situations were analyzed, three objects were investigate at first a constant load and a constant indentation depth. The three objects which were analyzed encompass the range of objects used in later simulations. A perfectly hemispherical object, the object with the smallest R value simulated and an object with an edge fillet to radius object ratio of 0.5. Figure 4 shows the results of these studies where x is the distance from the axi-symmetry line.

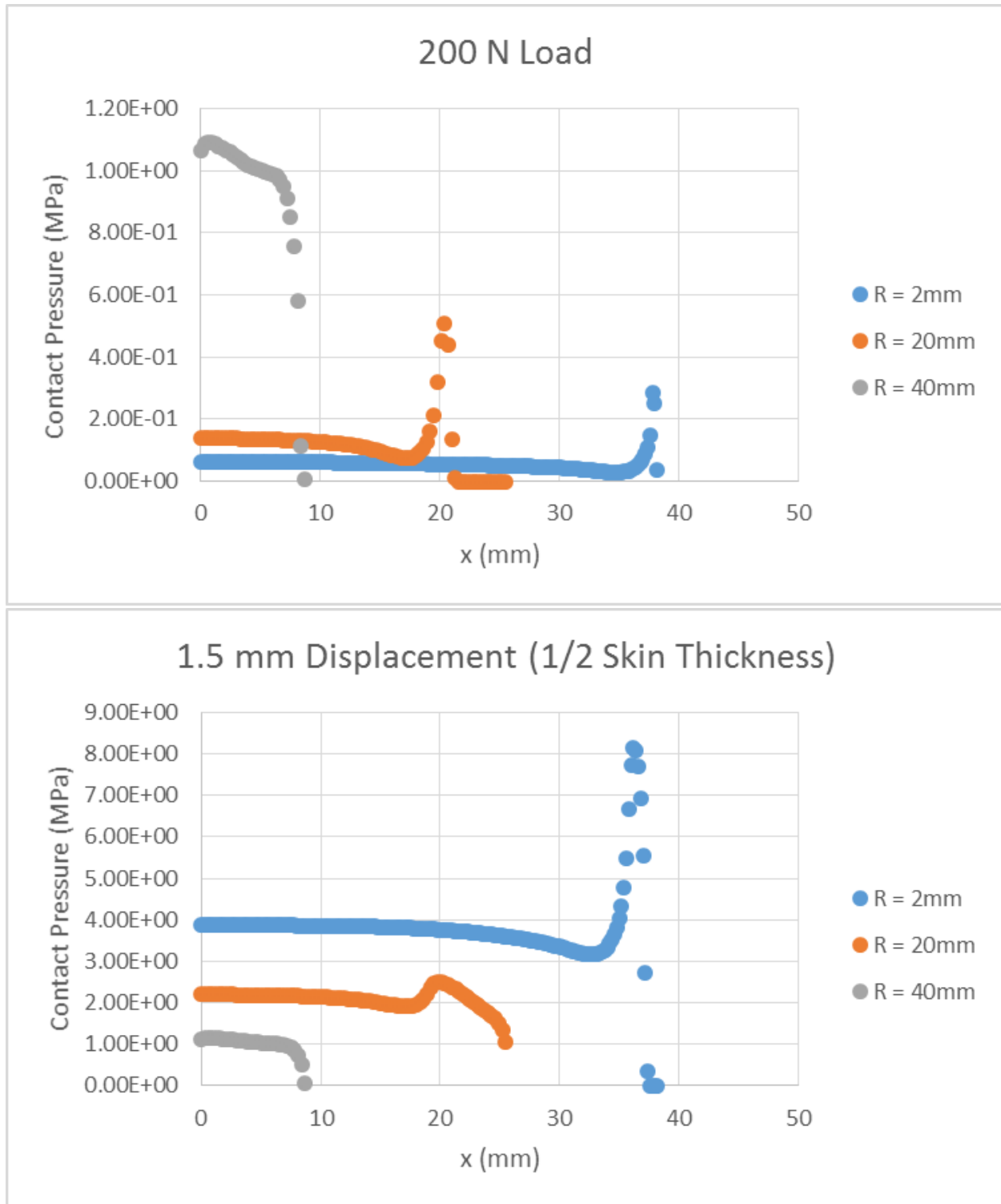


Figure 4. FEA Contact Pressure Distributions

As expected the hemispherical cap gives fairly close to a Hertzian contact pressure distribution. As the edge fillet decreases and the stresses peak around the part of the object where the fillet starts. Before this geometry feature, there is a drop in the pressure followed by a very tight spike in the contact pressure. These pressure distributes are what are expected and show correct formulation of the contact. When comparing the distributions at 200N of loading, the highest contact pressure is experienced during the hemispherical contact. As the filet radius decreases, the maximum pressure decreases and the initial dropoff is decreased in magnitude as well. This can be attributed to the increase in contact area due to the geometry of the object. However, this theory does not translate well when looking at the distributions at the same. When looking at the response for various objects in Figure 4, the increase in force to achieve a displacement as the object edge becomes sharp is significant. This also shows when examining the results shown in Figure 4. As the edge of the object sharpens, both the maximum and plateau contact pressures greatly increase. This is attributed to the overall increase force required as well as the stress approaching infinity for sharp edge contact. This focus of the research shows great promise as the mechanics of this contact is relatively unexplored especially with non-linear materials.

Another important aspect of the contact is what is commonly referred to as pile-up. This is a contact feature where the material near the edge of the object is pushed up and above the baseline height of the material. Looking at three different objects from hemispherical to nearly sharp edged, the amount of pile up is minimal. This can be seen in Figure 5 where all three models are shown at 3 mm of indentation depth, or the thickness of the skin layer. It is clear, that for all cases, little to no pile-up is present. This shows that during normal loading, there is almost no pinching of the tissue layers during the contact.

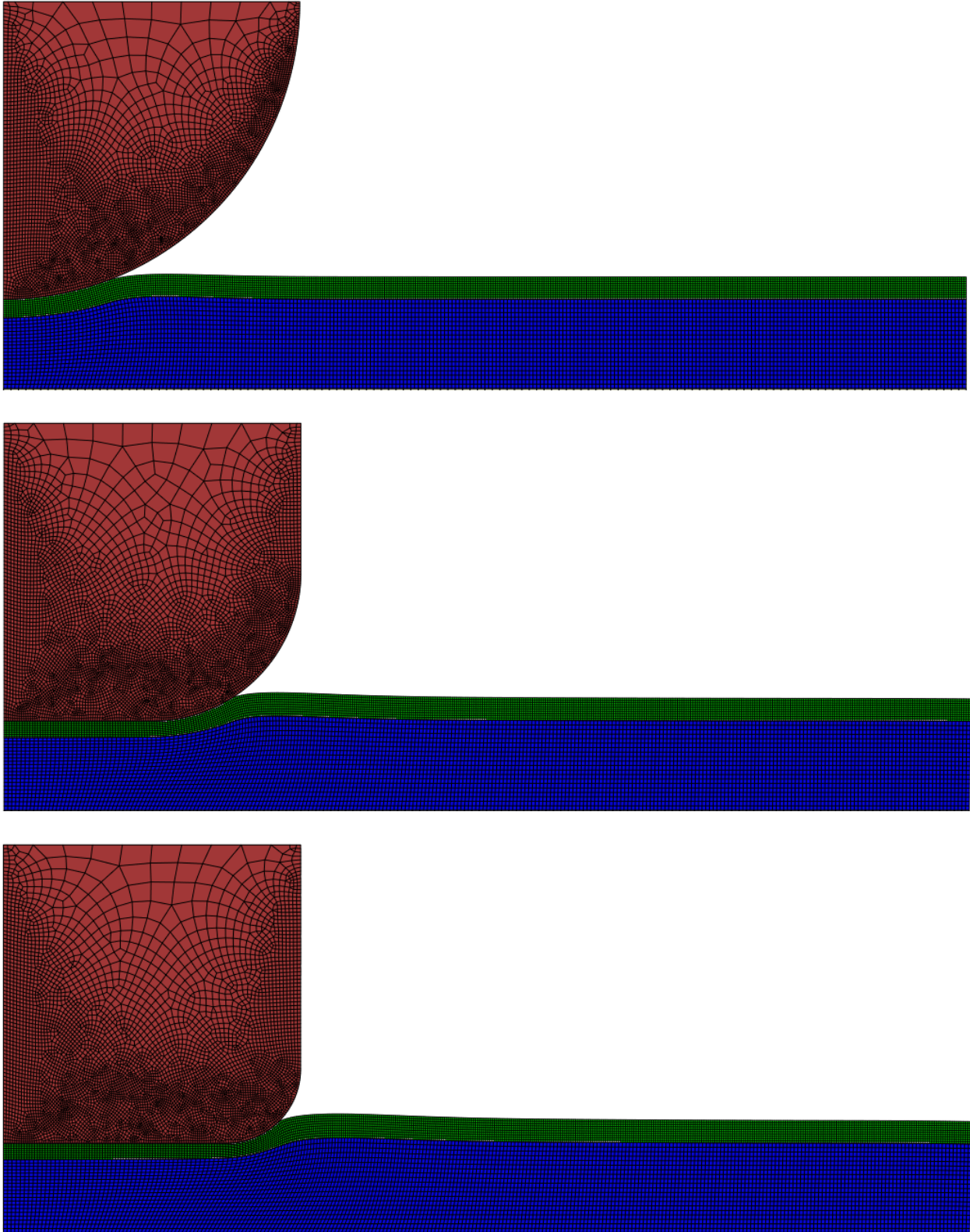


Figure 5. Indentation Pileup

Contusion Formation and Patterning

Using a strain based metric measuring maximum principal strain the contusion region was determined for the various FEA simulations. This is the best metric that is currently available for strain or stress based contusion measures when looking at general tissues under quasi-static loading. Other studies [7, 8], have looked at the rupture of a specifically orientated capillary which requires very specific assumptions about the area of interest.

From the simulations there are two major measures that show major trends in contusion formation and patterning. The first measurement is taken when there is the maximum principal strain exceeds 0.154 [3]. It is at this point that capillary damage can be expected. Although at this point, the contusion might not be visible on the surface of the skin damage will be present. The second measurement that was taken was when the contusion started to interact with the mid-plane of the model. For both of these measurements, both the energy and the energy over contact area were plotted. These plots can be seen with the in Figure 6.

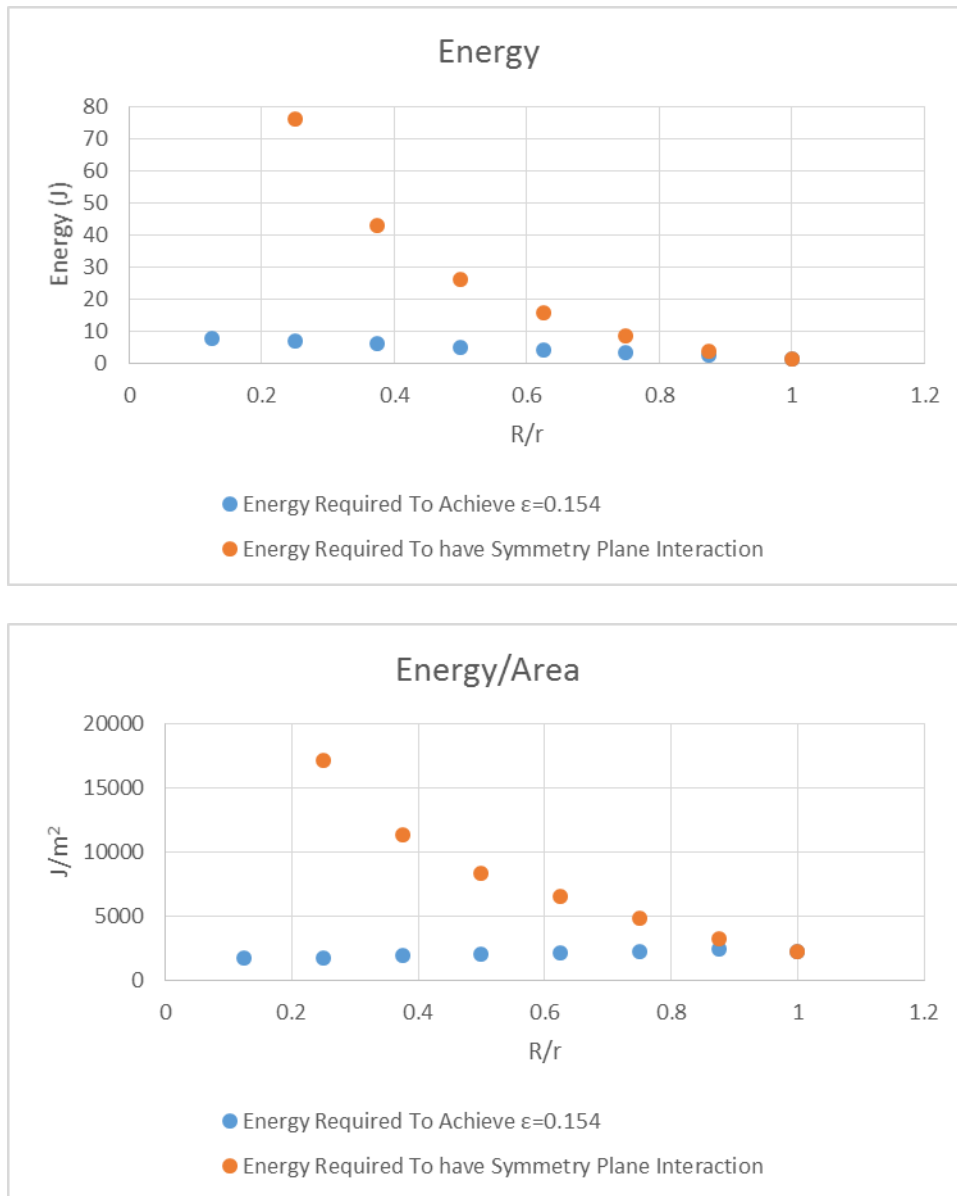


Figure 6. Contusion Energy Analysis

One of the first and most interesting things to note is that the trend for the start of the contusion change when the energy is divided by the contact area. For the energy plot, the trend shows that the energy to cause a contusion increases as the object approaches a sharp edge. However this slope is reversed when the energy is divided by the contact area. However, this change is relatively inconsequential and holds no bearing on how further analysis was conducted. Both of the plots show that when examining a specific energy value there will be contusions with

both defined edges and contusion which interact with the symmetry plane for a given object radius, r . The energy to reach the edge follows a fairly quadratic trend and this carries over to the curves energy over area curve.

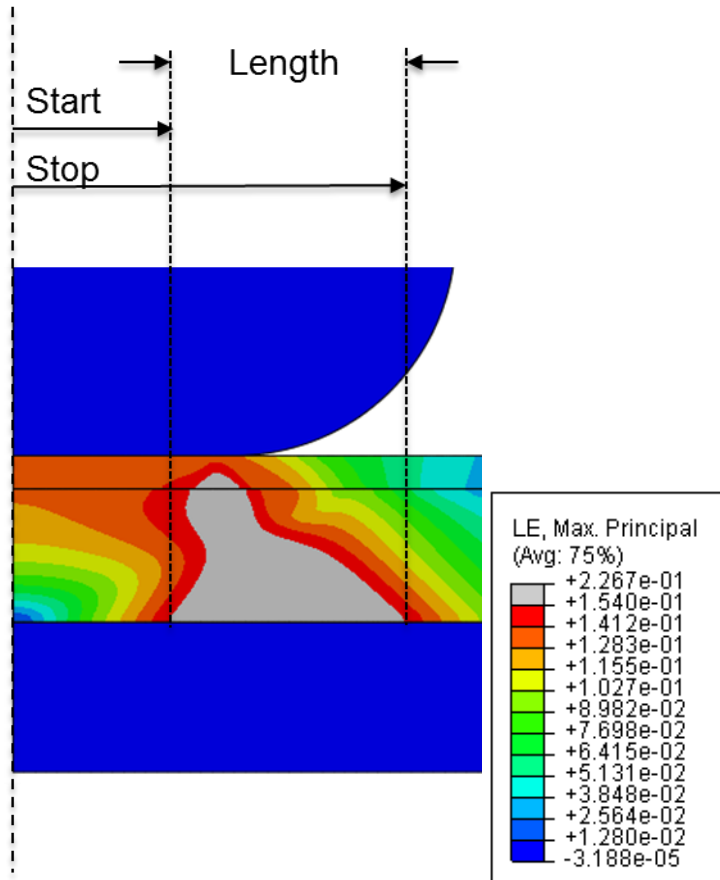


Figure 7. Contusion Measurements

There are two different ways that contusion evolution can be examined; at the same energy level across a sweep of objects and for a single object for several energy levels. The primary issue with looking across the same energy level is that to ensure contusions are present for all objects studies, there will be a part of the curve that shows the interaction with the mid-plane. This can be seen clearly in Figure 8.

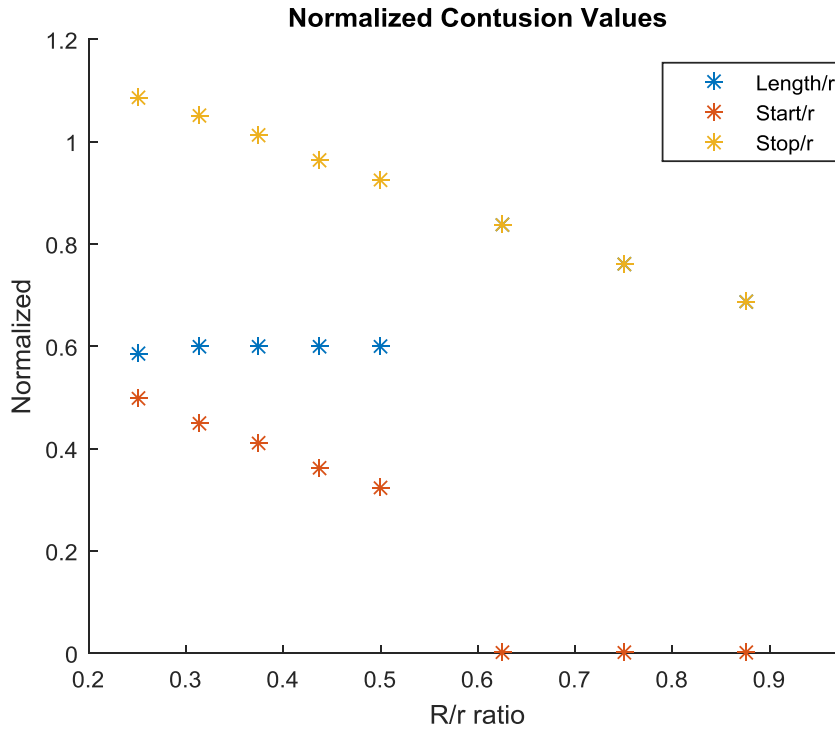


Figure 8. Contusion Dimensions

Before the point where there is mid-plane interaction, the inner and outer most points, as shown in Figure 7 of contusion change in a linear matter which means that the total length of the contusion is constant. When comparing the trends from Figure 8 with Figure 9, very different trends are evident which can lead to different inferences about the object. When looking at the same object for at multiple energy levels, the length of the contusion changes fairly linearly from contusion formation until the damaged region reaches the mid-plane. This shows that for a given level of damage and a known object, that energy levels required can be approximated. This is only true for flat capped punches as the hemispherical object patterns are quite different due to internal loading and the concentration of strain directly under the object.

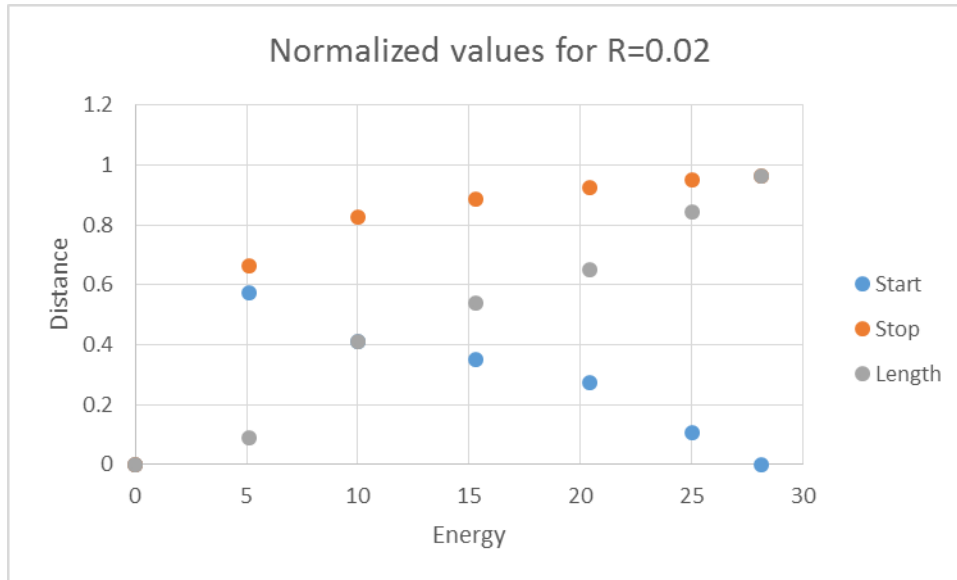


Figure 9. Contusion Dimensions for a Single Object

This work shows that the finite element method in conjunction with a basic measure for contusion region identification allows for insight into how contusions form and develop during the loading cycle. Object geometry was studied to show the dependence that this has not only on the shape of the contusion but also the response of the model. It is shown that for a given energy level or for a given object, it is possible to predict various quantities about the contusion shape and location.

CHAPTER 4: SHAFT LOADED BLISTER TEST

Introduction

The blister test best was developed as a method for testing the adhesion between thin films and the supporting substrate. First proposed by Dannenberg [21] and undergoing refinement by Malyshev and Salganik [22], the analytical models for this experiment have undergone serious advancements as more complex deformation models were used. It has been proven that basic beam theory cannot be used to develop accurate models for the fracture energy and the assumptions made have grave consequences on the accuracy of the solution. The early set-ups were known as pressurize blister test and use an incompressible fluid to apply uniform pressure to the film resulting in crack propagation along the interface. Measuring the pressure of the fluid and the displacement of the film allows for calculations of the fracture energy at the interface. A variation of this test is the shaft driven blister test (SLBT) where the fluid is replaced with a shaft used to apply load the film. The shafts control the load profile by and the distributions of pressure can be manipulated by changing the geometry. To get closer to a point load in the middle of the sample, a hemispherical cap punch is used while a flat-capped punch will allow for loading closer to the crack tip. This experiment is a displacement controlled experiment which allows for total failure to be avoided during testing.

The focus of the following studies will be on the shaft loaded blister tests exploring results for a theoretical point load solutions, and the validity of this solutions for flat capped shafts. Calculations for the fracture energy will be compared against FEA J-integral calculations for stationary crack models. Based on these findings, calculations will be done to verify these analytic models against the input for moving crack simulation. Finally, parametric studies will

be done conducted to see the effects that ice thickness, boundary conditions, substrate material, plug size, and crack length have on the required force to cause crack propagation.

Model Setup

The SLBT FEA model is composed of three major parts: the loading shaft, substrate, and ice layer. The model was create in an axi-symmetric environment since the plug being used is circular. This assumption allows a less complex and computationally inexpensive model. By simplifying the model significantly, the ability to run extensive parametric and design studies becomes significantly more time efficient. The basic geometry of the model is detailed in Figure 10 along with the various boundary conditions which were simulated.

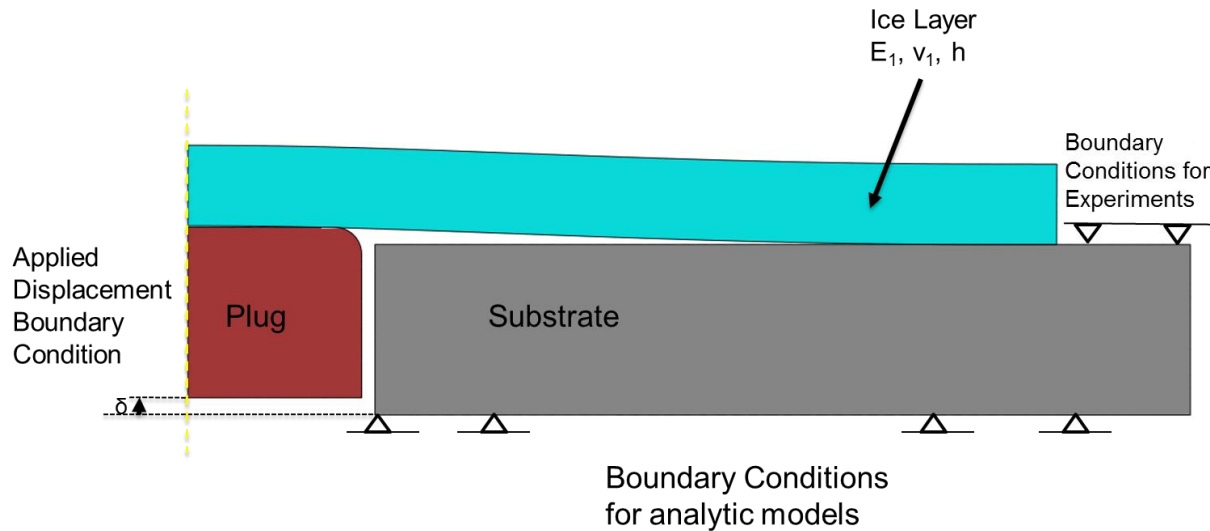


Figure 10. SLBT Geometry

To better try and match the basic analytical models in the literature, the base of the substrate was fully confined. These boundary conditions best simulate an infinite substrate which the models are based. When this model was transitioned to better simulate the boundary conditions found in the laboratory, a small top section of the substrate was constrained. In

addition to the different boundary conditions, several substrate materials were tested. Both Lexan and aluminum were used as substrates and the model responded quite differently which will be discussed in-depth later. The substrate material properties that were used are given in Table 4 along with the material properties for ice. In all following equations, when Young's Modulus and Poisson's Ratio are used they refer to the values for ice.

Table 4. SLBT Material Parameters

Material	Young's Modulus, E (GPA)	Poisson's Ratio ν
Ice	9.8	0.3
Lexan	24	0.37
Aluminum	70	0.33

To capture what is happening during a SLBT experiment requires the modelling of two interactions. Along the light blue line in Figure 11 hard, frictionless contact was used to model the interaction between the plug and ice. By doing this, the controlled displacement of the plug determines the loading in the ice layer. With an applied displacement boundary condition the plug will remain level during loading, and if the load was applied uniformly the plug would tilt during loading. Instead of making assumptions regarding the contact pressure profile between the plug and ice, assumptions are made in the numerical computation of the contact interaction which is a more reliable method. In doing this the model was made more general and has the ability to change between any of plug geometries and ice geometry. Finally, the bonding of ice to the substrate had to be modelled using CZM. The length of the initial crack was dictated by the where the slave and master surfaces are defined. The master surface was assigned to the substrate and the slave surface was assigned to the ice.

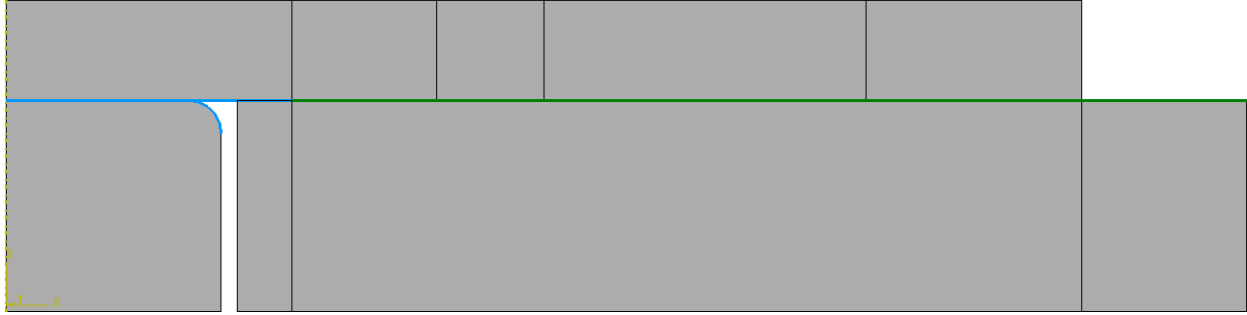


Figure 11. SLBT Interactions

To create the crack and allow for its propagation during simulation, cohesive zone modeling was used. Initially developed in the 1960's, the degree of damage at any point along the bond line can be determined based upon several parameters. In the below figure, a bi-linear cohesive zone model (CZM) which is what was used for all simulations. Once the peak traction was reached, the zone would start to be damaged with full debonding happening at the final separation.

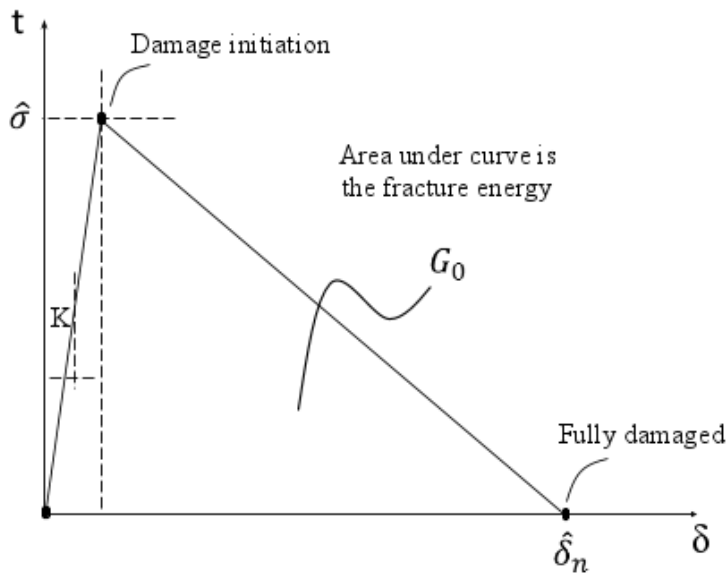


Figure 12. Bi-Linear Traction-Separation Curve

To determine the strength of the bond between the ice and substrate the fracture energy and the peak traction were specified. To determine the fracture energy, single cantilevered beam

samples were created and then tested using deadweights to apply the load. Using this load at failure and experimental geometry, it was calculated that the fracture energy of the system was approximately $4 \text{ J} / \text{m}^2$. The second parameter, peak traction, is a fitting parameter which in conjunction with the fracture energy determines the final separation and length of the cohesive zone. In addition to these two parameters, the slope of the left hand part, K , of the curve is inputted. For this analysis, this value is sufficiently large such that the CZM can be approximated as a right triangle. This leads to this simple equation to relate the fracture energy, maximum traction, and separation at complete failure.

$$G = \frac{1}{2} \hat{\sigma} \hat{\delta} \quad 4.1$$

Where

G =Fracture Energy

$\hat{\sigma}$ =Maximum Traction

$\hat{\delta}$ =Maximum Separation

In this type of modeling, the maximum traction is the best parameter that can be used to help shape the force-displacement curve. With the interface fracture energy being determined using single cantilever beam experiments, manipulating the maximum traction is an easy way to change the model response and properties which are dependent on the process zone size. By increasing the maximum traction, the damaged cohesive zone will shrink in size which helps

Stationary Crack Calculations

To first assess the viability of various analytic calculations for the fracture energy from a SLBT studies were done on stationary cracks were conducted and these values were compared to various analytical models. The analytical solutions are based upon the use of a theoretical point

load to deform the ice layer. To simulate this, a spherical shaft was used to best match this assumption. The base was large enough that insure no interaction between the stress fields caused by the crack and other interfaces. In addition to using both the force and displacement values from the FEM simulation, deflections were calculated using the equation [23,24].

$$\delta = \frac{3(1-\nu^2)PR^2}{4\pi Eh^3} \quad 4.2$$

Where

P=Applied Load

R=Crack Length

ν =Poisson's Ratio of Ice

E=Young's Modulus of Ice

h=Thickness of ice

For this study, the crack length was held at a constant 11.35mm and simulations were run for ice thicknesses of both 3 and 5 millimeters. This calculated displacement corresponds to the value at the top of the ice. From the simulation three displacement values can be taken and used; the displacement of the plug, displacement of the bottom of the ice, and the displacement of the top of the ice. These three displacements all show a different stories about what is happening during the simulation. The displacement of the plug is equivalent to the displacement data taken from experiments however the analytical models are not based off of this measurements. Due to how the models were derived, the displacement in the equations is the value that corresponds to displacement of the top of the ice. Much of this work is based how using the plug displacement changes the output of the solutions as that displacement can be experimental measured. Finally, the bottom of the ice can be measured which is uncommon to see used and impossible to

measure experimental. The differences in the displacement between the bottom and top of the ice layer shows the compression due to the loading.

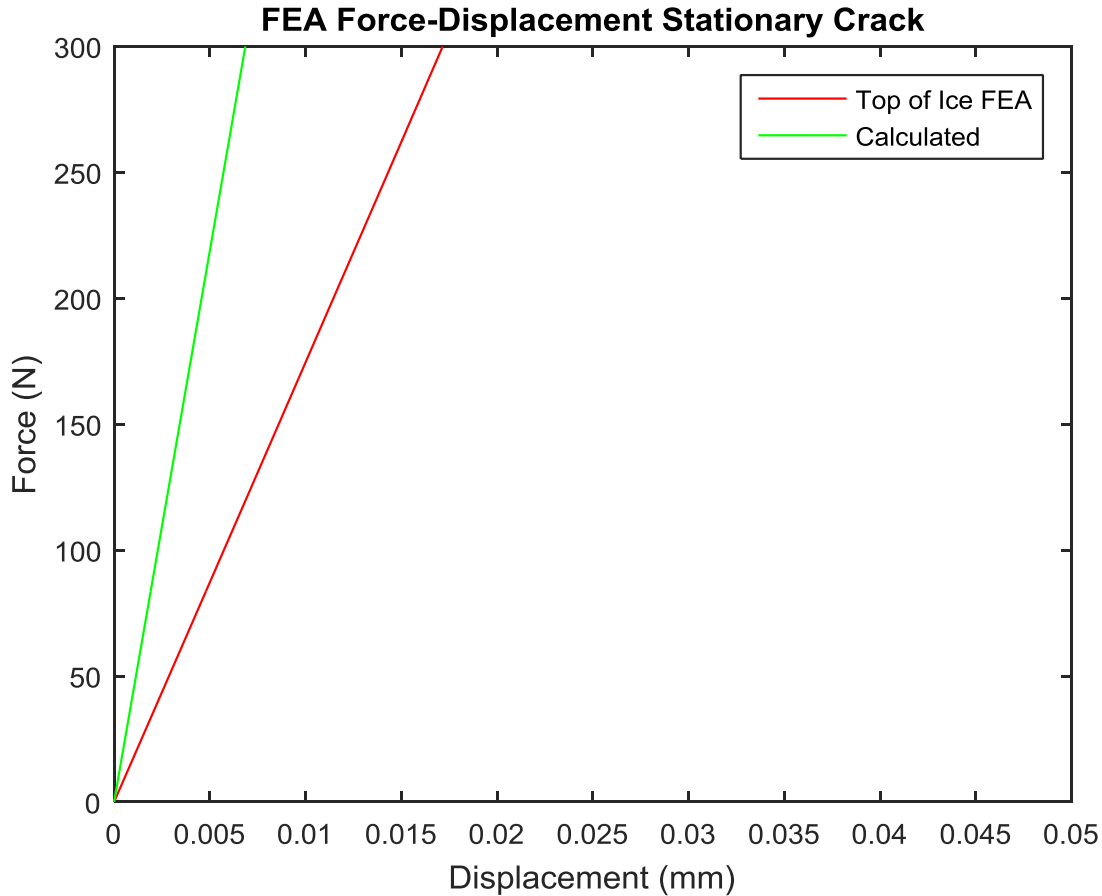


Figure 13. Calculated vs. FEA Displacement

With both ice thicknesses, the analytical model shows a much stiffer force-displacement interaction compared to the FEA. Overall, the 3mm ice runs show better agreement when compared to the 5mm sample and the results are shown in Figure 13. This can be attributed to the assumptions made when deriving the equation for the deflection. In those calculations, the ice was modelled as a thin film with a near-zero thickness. With all of this considered, the model shows relatively good agreement and will be examined more moving forward.

For the remainder of the study, two different expressions for the fracture energy were examined and compared to the J integral values that were extracted from the FEA simulations. The J integral is a path independent line integral which can be used to calculate energy release rate and fracture energy. Around a given path, Γ , the J integral can be defined using the following equation [25].

$$J = \int_{\Gamma} \left(w dy - T_i \frac{du_i}{dx} ds \right) \quad 4.3$$

where

w = strain energy density

T = traction vector

u = displacement

ds = length increment around contour

Carrying out these calculations in ABAQUS is computationally inexpensive and allows for comparison against analytical solutions. In ABAQUS multiple contours were defined to ensure path independence and it was found that after approximately 4 contours path independence was achieved and in the coming plots, the value from the 10th contour was plotted. For the analytic solutions that are being evaluated, the solutions from Hutchinson et al. and Jensen were selected. The Jensen solution [23] is

$$G = \frac{P\delta}{2\pi R^2} \quad 4.4$$

And the Hutchinson solution [24] is

$$G = \frac{2Eh^3\delta^2}{3(1-\nu^2)R^4} \quad 4.5$$

In Figure 13, there are three results plotted per graph. Both the Hutchison and Jensen solutions are evaluated for the available data using force, displacement and crack length from the FEM simulations. Both the plug displacement and the top of the ice displacement are used to determine the difference between the ideal displacement and what can be measured experimentally. These solutions are compared against the J integral values extracted from the FEA simulation. Plotted is a comparison of the values from the Jensen and Hutchinson calculations using the simulation displacements and the J integral results for 3mm thick ice.

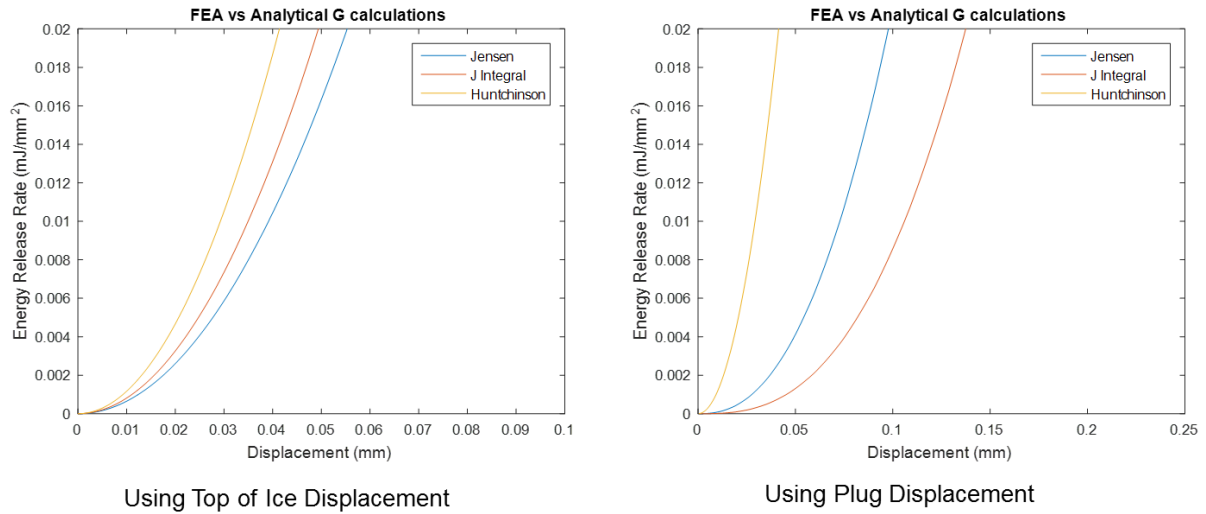


Figure 14. G Calculations with FEA Solution

The analytical solutions compare favorably with the FEA value with differing degrees of agreement based on the displacement used in the calculations. When the top of ice displacement from the finite element analysis is used, the solutions show very good agreement with the Hutchinson solution overestimating the value and Jensen underestimating. When the plug displacement is used, analogous to an experimentally measured displacement, both of the models over predict the fracture energy.

Moving Crack Calculations

Multiple basic analytical solutions will be compared to the expected values based on the input to the FEA model. The results of these calculations will be compared to the fracture energy that was inputted to define the CZM. As the crack propagates during the simulation, the calculations for G are expected to converge to a steady value of $4 \text{ J} / \text{m}^2$. To calculate the crack length from the simulations a cohesive damage parameter calculated by ABAQUS is used. When this parameter reaches a value of one the surfaces are taken to be fully separated. This analysis was carried out for two different values of maximum traction with $\hat{\sigma} = 0.1 \text{ MPa}$ and 1 MPa being used. This was done to assess how the shape of the traction-separation curve effected the accuracy of the solution for constant fracture energy which was experimentally determined. To first compare the effect this change had on the solution, the figure below shows the changes in the force-displacement curves. Both the displacement from the FEA simulations and calculated displacements are shown. This was also done to ensure that the code used to calculate the crack tip was correct. While both predict the curves to a relatively good degree of accuracy, it is interesting to note the curves for a maximum traction of 1 MPa generate a much closer fit. It is hypothesize that this is due to the reduction in the cohesive zone size and a move much closer to the small scale yielding approximation in fracture mechanics. The impact of this change on the model can be see clearly in Figure 15.

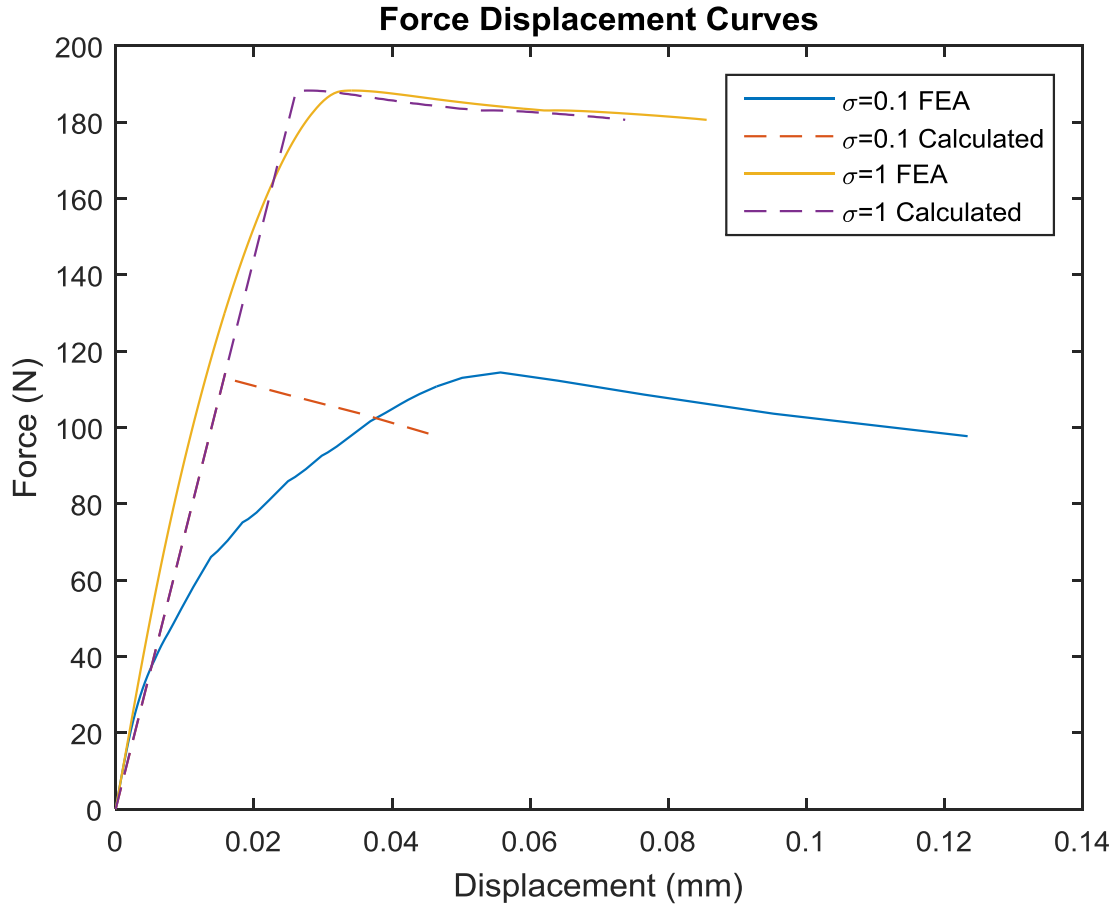


Figure 15. Model Response with Propagating Crack

The overall goal of this work is to develop and assess validity solutions that can be used when examining experimental data. To do this, the crack length needs to be removed from the equations since this cannot be measured easily using current experimental techniques. To do this, the calculation for displacement was substituted into the Hutchinson solution for the fracture energy. By doing this the equation for the fracture energy is now independent of the crack length.

$$G = \frac{P^2 3(1-\nu_1^2)}{8E_1 \pi^2 h^3} \quad 4.6$$

The results of using the finite element force and model parameters are shown in Figure 16, with the fracture energy being plotted against the plug displacement, the load, and the crack length.

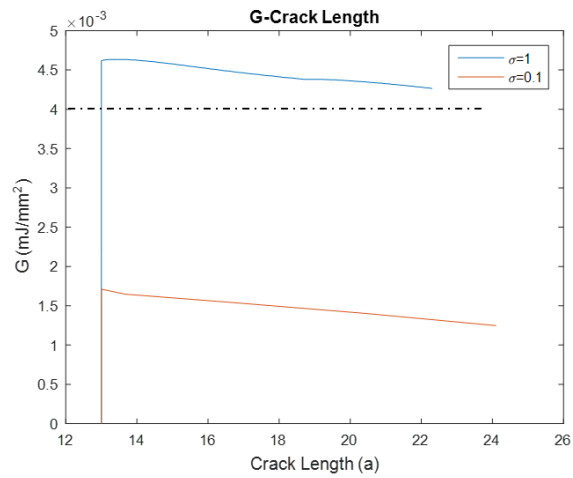
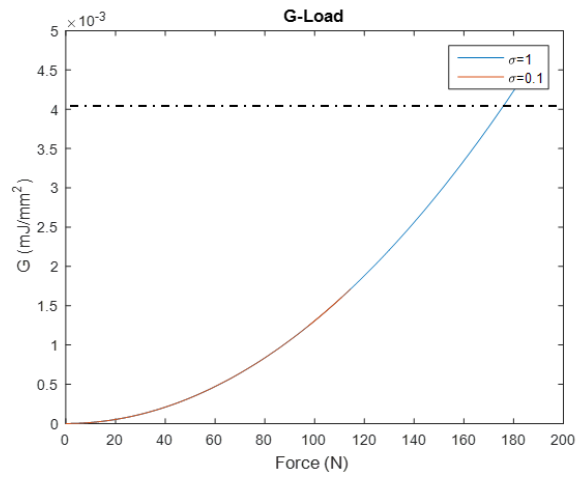
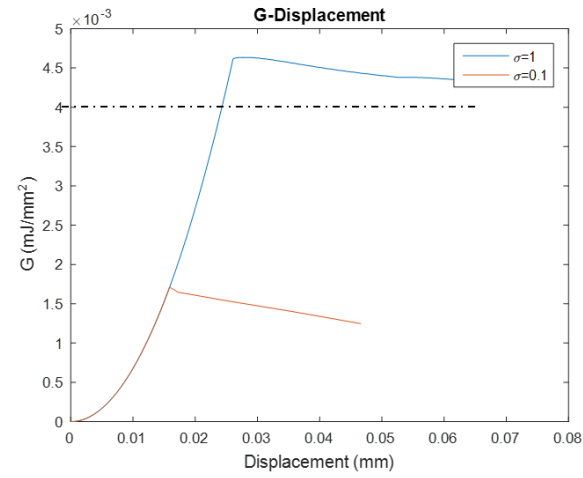


Figure 16. G Calculations for Propagating Crack

As expected based on examination of the force-displacement curves, the solutions for the simulations with a maximum traction of 1 MPa more accurately predicted the fracture energy. When the solutions are plotted against the displacement the trends become very clear. First, that when you use the calculated displacements for both the Hutchinson and Jensen solutions, the same results are obtained. The results can vary wildly based on the solution used and input of maximum traction. Results can be off by more than an order of magnitude or can be within 10% of the expected solution. With an increase in maximum traction, the results trend toward the model input value. From this analysis, the conclusion was reached that the solutions which use the calculated displacements show the best agreement with the expected value.

Parametric Studies

The final part of this preliminary study was to explore the effect that a variety of factors that affect the model response. This study was done to explore the effects slight changes will have on experiment design and response. The first major study was the effect that substrate material, ice thickness, and boundary conditions have on the response. In Figure 17, three plots are used to show the results of these simulations. The blue dots show the effects with an aluminum substrate with ideal substrate boundary conditions, orange shows aluminum with experimental constraints. Switching the substrate material over to Lexan the grey dots show the results for ideal boundary conditions and yellow shows the data pertaining to the experimental constraints. Although not shown in these plots, all thicknesses exhibited softening after the peak force was achieved.

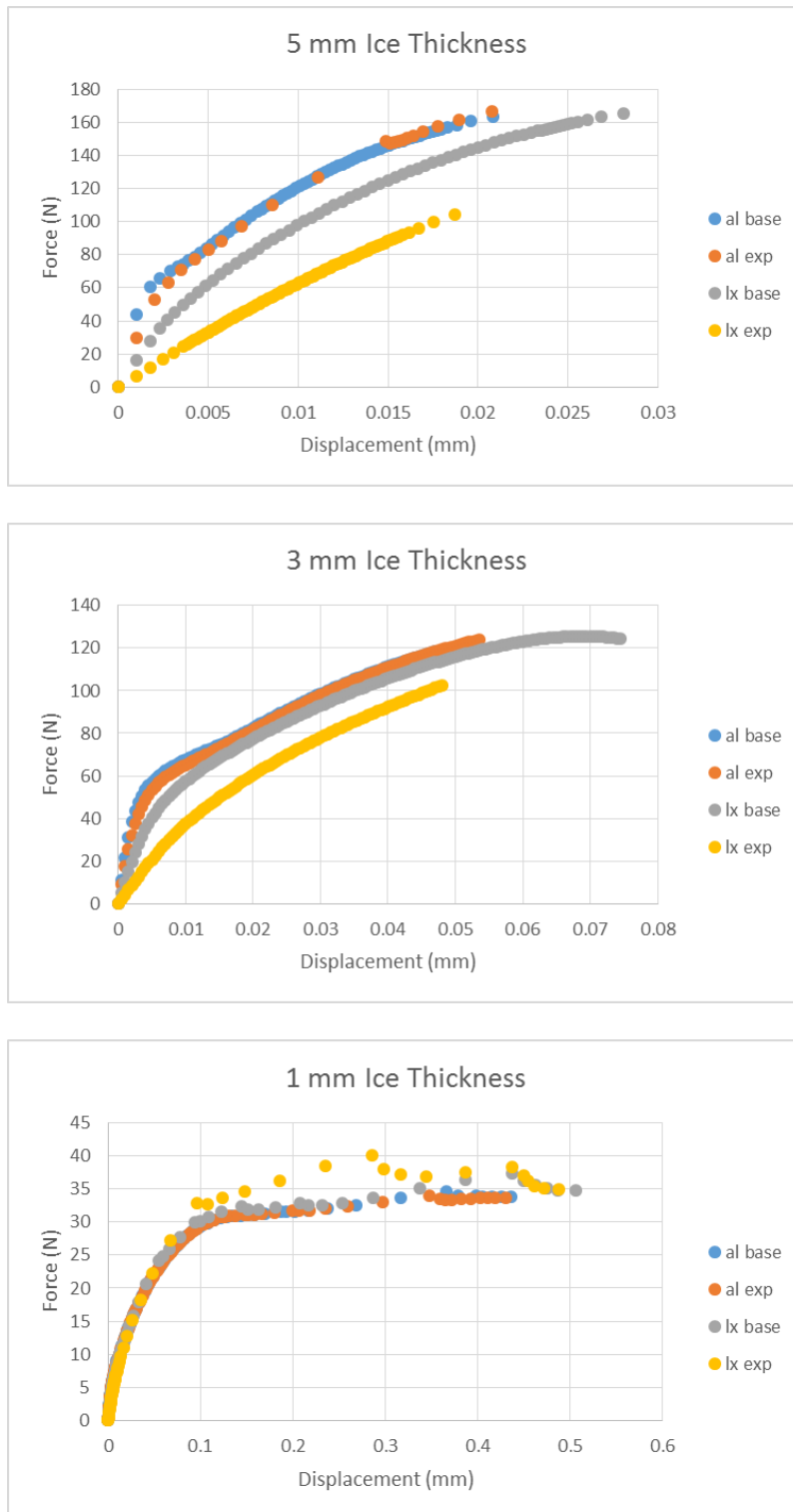


Figure 17. Parametric Sweep of Thickness, Substrate Material, and Boundary Conditions

There are several major takeaways from these plots which can inform and influence experimental design. As the ice layer gets thinner, the effects of substrate material selection and boundary conditions become inconsequential. This can be attributed to the decrease in force required to cause crack propagation. As ice layer thickness increases, these decisions start to have a much larger impact on the results. These results show the necessity to having accurate and consistent ice thicknesses when carrying out experimental analysis.

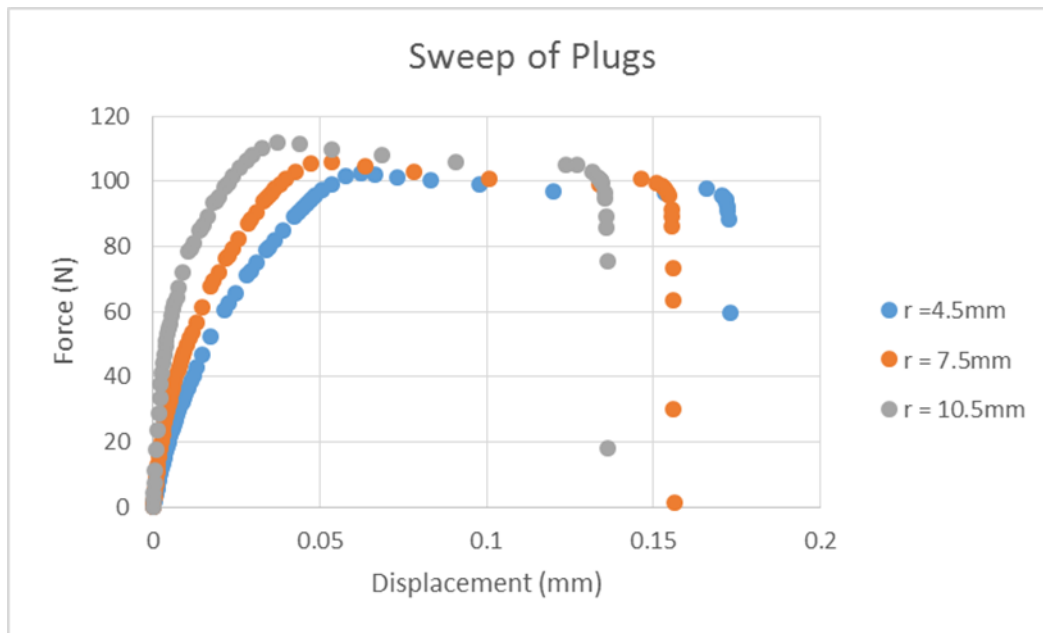


Figure 18. Parametric Sweep of Plug Radius

Next the effect of plug size was studied when the crack length was kept consistent. The results from these simulations can be found in Figure 18. The results of this test show the relative insensitivity of the model response when the plug changes shape. With a very large difference in plug geometry, the maximum force varies by only 10N and the displacements vary by less than half a millimeter.

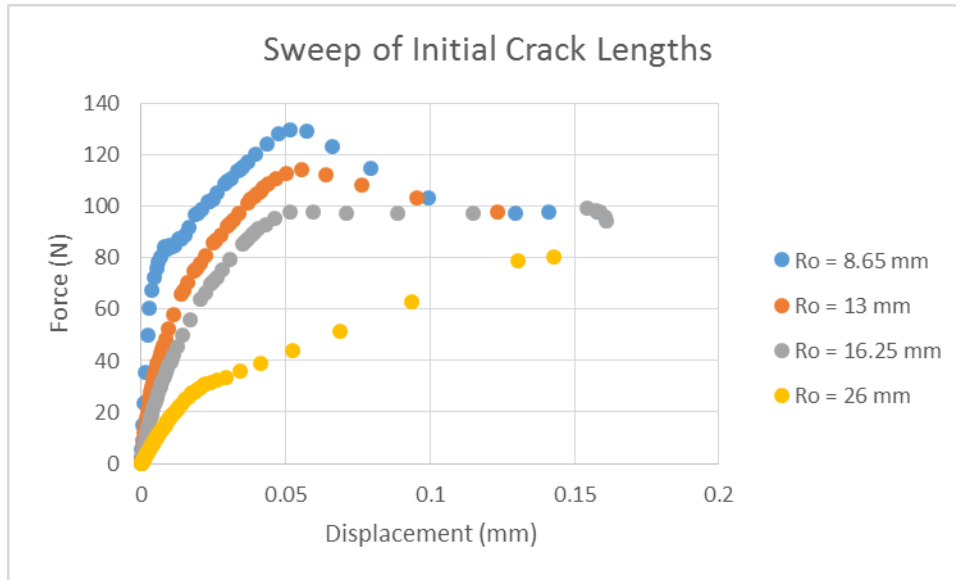


Figure 19. Parametric Sweep of Crack Length

Finally, the crack length was varied while the plug geometry was held constant. The results from this test can be found in Figure 19. Similar to the first parametric study, this shows the effects that non-consistent sample manufacturing has on response. Unlike with the plug geometry sweep, there is a massive effect on the maximum force required to propagate the crack. The biggest changes can be found when the initial crack length is very long. For the most part, there is only a 30N drop in maximum force but for the longest crack simulated the force drops drastically. This is due to the damage of the cohesive zone interacting with the edge of the ice layer very quickly. Overall, this works represents value decision making tools when determining the design of future experiments.

CHAPTER 5: CONCLUION

Summary

The FEA simulation environments which were created past part of this thesis work are basic testing setups which can now be modified for future use in more complex scenarios. With the simplicity allowed by using axisymmetric models, basic contact mechanics and using layered models, a basic understanding of how different parameters effect model performance was gained during parametric evaluations. By doing this type of model development, understanding can be attained without having to worry about how various factors, such as sharp corners or interactions with edges, affect parametric studies being studied. These FEA models and the practices developed during the creation of them will allow for easy comparison against experimental data and analytic model validation.

When examining the current literature for current methods of solving the problems presented in this thesis both the analytic and numerical models used are highly case specific. In the contusion research, the vast majority of simulations were based on patient specific models which only apply to a small slice of the patient. While useful for proving the validity of models, to date no studies have looked at how damage propagates in a basic system. While being around for more than 50 years, the work done currently on the SLBT is again designed to be highly specific and case sensitive. As proven, the most basic models can be used to predict accurately predict the fracture energy with limited data. Both of these models main purposes is to be used in further work as more specific cases can be examined and experimental data can be used to validate.

Simulation Uses

These simulation environments have been developed with the purpose of use for comparisons against experimental data and using experimental data to compare with the simulated values. The goal of making these models as general was so that only minimal changes would need to be made in order to better replicate the experiment or situations in the simulation. By doing this, the user will only need to change a couple of input values and dimensions to completely change the simulation to reflect the specific case being studied. This allows for time and effort to be saved by working in a proven simulation environment with validated methods and techniques.

This work diverges from the literature by going to great lengths and making a great effort to be as general as possible. As previously stated, for both the contusion studies and SLBT solutions, the literature tends to work with highly case specific models where the work being done does not transfer over to new problems. This work represents the first steps of using very general models and analytic solutions to describe the mechanics of the problem.

The intended use of these environments is to develop a base knowledge of the problem being studied before moving to more specific models to fine tune computational data. This has been done by creating environments that can be examined in great depth with only a couple of parametric studies. For the work being done with SLBT, the model has been designed to work in conjunction with laboratory experiments and work together to validate both the simulation and analytic models.

Simulation Limitations

Unfortunately no tool is perfect and these simulation environments no expectations. As with any simulation development had to be made in order to get it running and solving the desired problems. Before discussing the limitations of the physics being used, assumptions were made about the contact and how the load was transferred during the simulation. It was assumed that the contact was both hard and frictionless, an assumption commonly made during simulation but experimental impossible. The effects of changing this are currently unknown and have not be studied at this time. In the contusion work two major assumptions were made that limit the tool. The first being that the impact was at a high rate which effects the material properties being used. Without using an explicit solver and a specific situation with a known velocity, this poses serious limitations on the scenarios that can be studied. Secondly and perhaps the biggest, the use of a metric based off of rat lung damage limits the work done. Unfortunately without enormous amounts of testing data from human subjects, this will have to serve as the best available metric for now. For the SLBT work, the biggest limitation is using a standard FEA solver with a bilinear traction separation zone to model the interface. This does not take into account the ways that cracks can kink into the ice layer as well as the type of fracture which is happening along the interface. However, this work is not designed to investigate this type of fracture and for the purpose of validating analytic solutions for the fracture energy, this model preforms as intended.

Future Work

The work done in this thesis represents the start of the work which will be continued for the next several years in many capacities. As this work progresses both problems will have aspects studied in greater detail. For the contusion work, the simulation environment will be

updated as more data becomes available and the field is advanced. As well, this work provides an area of research not frequently studied such as contact with non-linear materials and how these materials behave when in a serial configuration. The next steps for the SLBT model is multi-pronged, updating properties with experimental results and examining other fracture phenomena such as mixed mode fracture. Using data acquired from tests whose properties were determined based off of the parametric studies, the model will be updated to reflect real world fracture mechanics not previously taken into account.

BIBLIOGRAPHY

1. Ciavarella M., Hills D. A., Monno G., The influence of rounded edges on indentation by a flat punch, *Proc Instn Mech Engrs*, 1997, 212
2. Spilsbury B., The medico-legal significance of bruises. *Med Legal, Crim Rev.* 1937; 7:215– 27.
3. Gayzik F. S., Hoth J. J., Daly M., Meredith J. W., Stitzel J. D., A Finite Element-Based Injury Metric for Pulmonary Contusion: Investigation of Candidate Metrics Through Correlation with Computed Tomography, *Stapp Car Crash J*, 2007; 51: 189-209.
4. Shergold O.A., Fleck N.A., Mechanism of deep penetration of soft solids, with application to the injection and wounding of skin, *Proc Roy Soc Lond A*, 2004; 460:3037–58.
5. Shergold O.A., Fleck N.A., Experimental investigation into the deep penetration of soft solids by sharp and blunt punches, with application to the piercing of skin, *Trans ASME*, 2005; 127:838–48.
6. Linder-Ganz E., Shabshin N., Gefen A., Patient-specific modeling of deep tissue injury biomechanics in an unconscious patient who developed myonecrosis after prolonged lying, *J Tissue Viability*, 2009; 18.
7. Huang L., Bakker N., Kim J., Marston J., Grosse I., Tis J., and Cullinane D., A Multi-Scale Finite Element Model of Bruising in Soft Connective Tissues, *J Forensic Biomech*, 2012; 3.
8. Grosse I.R., Huang L., Davis J.L., Cullinane D., A Multilevel Hierarchical Finite Element Model for Capillary Failure in Soft Tissue, *J. Biomechanical Engineering*, 2014; 136.
9. Payne T., Mitchell S., Bibb R., Waters M., The Evaluation of New Multi-Material Human Soft Tissue Simulants for Sports Impact Surrogates, *J. Mechanical Behavior of Biomedical Materials*, 2015, 41
10. Ogden R.W., 1984 *Non-Linear Elastic Deformations*, Dover Civil and Mechanical Engineering.

11. Comley K., Fleck N., The Compressive Response of Porcine Adipose Tissue from Low to High Strain Rate, *Int. J. Impact Engineering*, 2012,46
12. Shergold O. A., Fleck N. A., Radfor D., The Uniaxial Stress Versus Strain Response of Pig Skin and Silicone Rubber at Low and High Strain Rates, *Int. J. Impact Engineering*, 2006,32
13. Shen W., Niu Y., Mattrey R. F., Fournier A., Corbeil J., Kono Yuko., Stuhmiller J H., Development and Validation of Subject-Specific Finite Element Models for Blunt Trauma Study, *J. Biomechanical Engineering*, 2008, 130
14. Roberts J. C., Biermann P. J., O'Connor J. V., Ward E. E., Cain R. P., Carkhuff B. G., Merkle A. C., Modeling Nonpenetrating Ballistic Impact on a Human Torso, *Johns Hopkins APL Tech Digest*, 2005, 26
15. Desmoulin G. T., Anderson G. S., Method to investigate contusion mechanics in living humans, *J Forensic Biomech*, 2011; 2.
16. Pilling M.L., Vanezis P., Perrett D., Johnston A., Visual assessment of the timing of bruising by forensic experts, *J of Forensic and Legal Medicine*, 2010; 17(3):143-149.
17. Thali M.J., Braun M., Brueschweiler W., Dirnhofer R., 'Morphological imprint': determination of the injury-causing weapon from the wound morphology using forensic 3D/CAD-supported photogrammetry, *Forensic Science International*, 2003; 132(3): 177-181.
18. Thali M., Kneubeul B., Dirnhofer R., A skin-skull-brain model for the biomechanical reconstruction of blunt forces to the human head, *Forensic Sci Int*, 2002; 125:195–200.
19. Stam B., van Gemert M. J. C., van Leeuwen T. G., Aalders M. C. G., 3D Finite Compartment Modeling of Formation and Healing of Bruises may Identify Methods for Age Determination of Bruises, *Med Biol Eng Comput*, 2010, 48
20. Morse C.I., Tolfrey K., Thom J.M., Vassilopoulos V., Maganaris C.N., Narici M.V., Gastrocnemius muscle specific forces in boys and men, *J Applied Physiology*, 2008; 104.
21. Dannenber H., Measurement of Adhesion by a Blister Method, *J. Applied Polymer Science*, 1961, 5

22. Malyshev B. M., Salganik R. L., The Strength of Adhesive Joints Using the Theory of Cracks, Int J. of Fracture, 1965 1,
23. Jensen H. M., The Blister Test for Interface Toughness Measurement, Engineering Fracture Mechanics, 1991, 40
24. Hutchinson J. W., Suo Z., Mixed Mode Cracking in Layered Materials, Advances Applied Mechanics, 1992, 29
25. Anderson T. L., 2005 Fracture Mechanics Fundamentals and Applications, CRC